






Communication Delay in UAV Missions: A Controller Gain Analysis to Improve Flight Stability

Leonardo A. Fagundes-Júnior , André F. Coelho , Daniel K. D. Villa ,
Mario Sarcinelli-Filho , and Alexandre S. Brandão 

Abstract—In real-world applications involving unmanned aerial vehicles (UAVs) the presence of communication delays can deteriorate the performance of flight control system or even cause instabilities. However, it is possible to improve the performance and ensure flight stability in the task execution by properly controlling the UAV considering the transport delay. This work analyzes the asymptotic convergence of a quadrotor, under time-delay in the communication with a ground control station. The effects of the communication delay, as well as the response-signal behavior of the quadrotors in the accomplishment of positioning missions are presented and analyzed by numerical simulations. The performance indexes (IAE and ITAE) assist the estimation of the acceptable time-delay limit. The results show that the adopted controller, without any adaptive tuning, can handle a delay of up to 1.2 seconds, which means a blind time of 40 packets of information. As expected, the longer the delay, the lower the gains. Consequently, as the delay increases, the quadrotor takes longer to accomplish the mission carefully and successfully.

Index Terms—Time-Delayed Control; Gain-schedule Analysis; Performance Indexes; Communication Delay; Aerial robotics.

I. INTRODUCTION

The problem of robot control is associated with its stability and performance during a task execution. Due to the discretization of controllers and the need for communication among robots and a ground control station (GCS), there is a certain time-delay in sending and receiving data [1]. Due to the limitations of wireless networks, controlled navigation using such a communication link is indeed a challenge. The presence of delays, besides being a difficult task to model and handle, can cause performance deterioration or even loss of stability of the entire system [2].

The delay comes from different sources, such as the inherent characteristics of the robot components (sensor and actuator dynamic response), data acquisition and processing systems, limited processing and transmission capacity, among others. It is worth noting that depending on its averaging time, it can distort the input commands and/or the sensor data.

L. A. Fagundes-Júnior and A. S. Brandão are with the Núcleo de Especialização em Robótica, Department of Electrical Engineering, and Graduate Program on Computer Science, Universidade Federal de Viçosa, Viçosa - MG, Brazil, Emails: leonardo.fagundes@ufv.br and alexandre.brandao@ufv.br

A. F. Coelho is with Institute of Robotics and Mechatronics, German Aerospace Center (DLR), Wessling, Germany. Email: andre.coelho@dlr.de

D. K. D. Villa and M. Sarcinelli-Filho are with the Department of Electrical Engineering, Graduate Program on Electrical Engineering, Universidade Federal do Espírito Santo, Vitória - ES, Brazil, where Mr. Villa is pursuing a PhD degree. Emails: danielkdv@gmail.com and mario.sarcinelli@ufes.br

A. Time Delay in Aerial Robots

The tracking control of mobile robots under communication network circumstances and limitations has attracted considerable attention from the scientific community and has been extensively investigated in recent years [1]–[4]. The authors present the problem of controlling robots from a GCS. The problem becomes more complex especially in outdoor environments due to losses in the quality of the communication link. For robot formation control, time domain passivity control techniques stabilize the cooperative landing of an unmanned aerial vehicle (UAV) on a moving ground vehicle through communication delays and packet loss, under delays up to 4 seconds [5].

In teleoperation systems, delays can compromise the margins of transparency and stability, which must be maintained to ensure smooth operation of the system and provide adequate kinesthetic sensation to the human operator. In [6], the stability for bilateral teleoperation control is guaranteed while removing position drift under unknown time-varying communication delay. In such work, the authors proposed a method to decouple the agents (master and slave ones), in such a way that one of them directly influences the other. It can be achieved by introducing a proxy agent into the architecture, to track the delayed information as accurately as possible. Consequently the transparency between the two agents is enhanced.

The practical design issues of continuous-time-delayed control (TDC) is addressed in [7]. This control methodology is recognized for its robust performance and simplicity in form, however it requires a state feedback that may not be available explicitly in some cases or it is corrupted due to the uncertainties of sensing and communication systems. The proposed technique eliminates the explicit requirement of velocity and acceleration feedback, and uses only position information from present and past instances with their respective timestamps, in order to mitigate the measurement error arising from numerical derivations cause by the time delay.

When the delay is variant, one can observe more intense problems regarding the stability of the system. The authors in [8] developed techniques for cooperation control of aerial robots under time delay based on leader-follower formation strategy. When neighboring positions and speeds are available, a control protocol based on linear systems is created, enabling formation maneuvers even with time-varying delays. Regardless of the number of agents, the formation maintains the leader-follower characteristic so that these followers can

track the time-varying references accurately and continuously throughout performed task. The stability analysis is demonstrated in the sense of Lyapunov-Krasovskii (an extension of Lyapunov stability theory for time-delay systems).

Given the imperfections in communication networks, traditional control strategies prove ineffective in some situations. Therefore, some modifications are required to deal with emerging challenges such as delays, packet loss, and limited bandwidth. The successful execution of a task is mainly dictated by the behavior of the implemented controller, the instrumental framework, and the response time of all of them. In the literature, there are still few works that propose to study the behavior of UAVs under communication delay in their control designs [9]–[14].

B. Work Contributions

In the literature, most proposed controllers do not consider the effects of delay in sending and receiving information. In certain scenarios, it is important to analyze the application limits of these controllers in the face of real physical systems and their intrinsic delays, and then seek the development of specific techniques to mitigate the loss of quality in the execution of the task.

In this scientific gap, this work aims to analyze the influence of communication delay on asymptotic convergence and stability of a quadrotor UAV, during a regulation task. In order to verify the limits of stable operation, this work aims to study the effects of the delay between getting sensory information and sending control signals, knowing that the proposed controller does not take the delay parameter into account.

The main contribution of this work is the proposed methodology to analyze and tune controller gains considering the existence of communication delay. The adopted approach implements an analysis in the parameter space [15] considering the two control gains and a fixed time delay, i.e. a three-dimensional search space. From the analysis, a surface is generated in which we consider that the robot can navigate and complete the mission and converge to the target point in a stable and timely manner. The calibration of the controller gains can then be performed from the generated volume, since it is guaranteed that in this region, the robot will not oscillate with increasing amplitude, destabilizing its movement. To validate this methodology, the work also presents a control structure that takes into account the delay in sending information from the robot to the control system. For this, the AuRoRA¹ platform validates the proposed control scheme and analyzes the dynamic behavior of the UAV under the input delay conditions.

The rest of the article is organized as follows. Section II introduces the mathematical model of the UAV. Then, Section III presents the formulation of the communication delay problem and the analysis approach in parametric control space. Next, Section IV shows the results obtained through numerical experiments, in order to evaluate the proposed control scheme. Finally, the conclusion remarks and suggestions for future work are depicted in Section V.

II. MODELING AND CONTROL

The quadrotor shown in Figure 1(a) is the AR.Drone 2.0, Parrot Drones SAS, and it is the UAV chosen for this research. It consists of a set of four independently driven cross-shaped motors. The collective variation of the propellers govern the three-dimensional navigation of the aircraft. Two opposing engines rotate clockwise while the other two rotate counterclockwise, a configuration that eliminates the anti-torque effect on the fuselage caused by the rotation of the engine blades (as shown in Figure 1(b)). There is also a low-level internal controller responsible for takeoff, hovering and landing [16]. This flight machine has six degrees of freedom (DOF), as shown in Figure 2. Three of them determine the UAV position, while the remaining ones describe its attitude. All of them are represented in the inertial frame $\langle w \rangle$.

The UAV control is an under-actuated one, since this machine has less actuators than DoFs [17]–[19]. The command signals sent to guide it [20] are $\mathbf{u} = [u_\phi \ u_\theta \ u_z \ u_\psi]^\top \in [-1, 1]$, where u_ϕ controls the roll angle, responsible for the left-right movement; u_θ controls the pitch angle, which results in forward and backward movement u_z controls the vertical velocity, or normal displacements; u_ψ is responsible for the yaw rate, which rotates the robot around its own z -axis. Such control signals are normalized and corrected to values proportional to the maximum roll and pitch angles, as well as the maximum vertical displacement and yaw rates.

For displacements at low velocities subject to the minimal action of external disturbances, the kinematic model of the UAV is enough to describe its behavior during flight. This assumption is only valid for navigation in a controlled environment such that UAV dynamic effects can be neglected. Otherwise, since quadrotors have an inherently unstable and highly coupled nonlinear dynamic model, their dynamics must be considered when designing controllers [17]. Respecting such conditions, without loss of generality, controllers similar to the ones presented in [16], [17], [21], [22] can be designed and implemented.

The UAV posture in generalized coordinate vector is $\mathbf{x} = [\xi^\top \ \eta^\top]^\top = [x \ y \ z \ \phi \ \theta \ \psi]^\top$, where $\xi \in \eta \in \mathbb{R}^3$ are the position and orientation vectors of the robot, respectively. The first one, $\xi = [x \ y \ z]^\top$ corresponds to the longitudinal, lateral and normal displacements, and $\eta = [\phi \ \theta \ \psi]^\top$ corresponds to

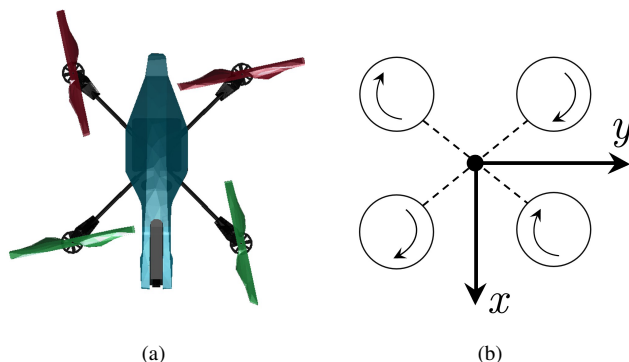


Fig. 1. Representation of (a) the aerial robot used, and (b) display of the blade drive configuration.

¹<https://github.com/neroUFV>

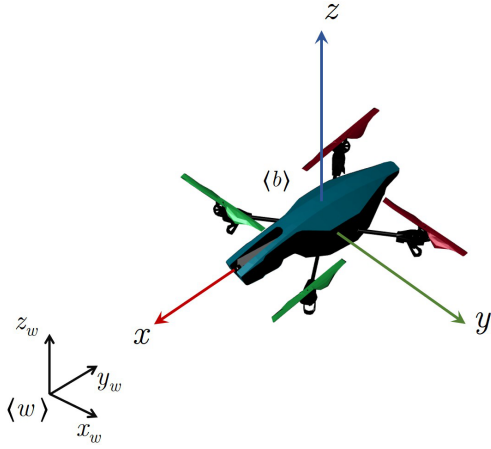


Fig. 2. Description and pose variables of the ArDrone 2.0 $\langle b \rangle$ in respect of the inertial frame $\langle w \rangle$.

the Tait-Bryan angles. The parameters of the dynamic model of the UAV are available in [17].

It is worth stressing that the focus of this work is not the proposal of a new control strategy. Indeed, the current objective aims to empirically verify the closed-loop stability as the delay time of the feedback control increases, for our already designed controller [17].

III. ANALYSIS IN THE PARAMETER SPACE

In this work we start with an analysis of the controller behavior, neglecting the effects caused by time-delay during sending and receiving information. In the sequence, we observe the UAV response in the face of the time-delay, after tuning its gains. Finally, knowing the maximum delay that guarantees the UAV stability, we predict its behavior as the time-delay increases and the controller gains remain constant. This prediction is achieved through the knowledge of the behavior profile of the controller parameters (gains) according to the increase of the time delay. Thus, for a given value of communication time delay, it is possible to estimate the behavior of the robot, which is stable if the chosen combination of parameters is within a volume comprising all possible gains that stabilize the robot. This conclusion is the result of this proposal, and it can be easily extended to different missions or robot models.

A. Controller Subject to Time-Delay

Let's consider the UAV model as a double integrator, so the control inputs are now related to $\mathbf{d} = [\ddot{x} \ \ddot{y} \ \ddot{z}]^T$.

Remark 1: The variable \mathbf{d} represents the delayed version of \mathbf{x} . In other words, \mathbf{d} stores the running data for further analysis, or gets the data delayed due to the communication delay that occurs in practical applications.

Remark 2: While \mathbf{x} has the current states of the UAV, \mathbf{d} stores the data for the entire mission. Thus, using the latter set, it is possible to emulate a delay time scenario. Furthermore, it allows you to analyze the communication delay time when sending a control input or receiving sensor data.

The GCS is responsible for receiving the data from the UAV, computing the control signals, and sending them via wireless communication. Once it is known that the under-actuated nonlinear controller runs on the GCS, the communication link with the UAV can present several problems that may cause time delay, such as the shadow effect, interference from other devices communicating on the same channel or close bandwidths, signal losses due to increased UAV-GCS distance, and others.

Figure 3 illustrates the control flowchart used to validate this work. Notice that there is a wireless link between the UAV and the GCS. In addition, the current states of the UAV \mathbf{x} , $\dot{\mathbf{x}}$ and $\ddot{\mathbf{x}}$ are available to calculate the errors required by the control law. It is assumed that the adopted communication system causes a bidirectional delay.

For all simulations, the reference control signals are tracked by the UAV. Its dynamic model is represented in gray in Figure 3 and detailed in [17]. This model does not consider any time delay on its design. In other words, the robot sees and navigates the world at its current stage. Again, it is worth noting that \mathbf{x} has the current data of the UAV, and \mathbf{d} has the history data, that can be labeled for any passed fixed time t_k .

Figure 3 also illustrates the control loop used, with the desired posture \mathbf{x}_d (constant for the positioning task, and time-varying for the trajectory tracking task), $\dot{\mathbf{x}}$ and $\ddot{\mathbf{x}}$ representing velocity and acceleration, respectively.

Considering the discretization of the system, the delay in receiving and sending information is represented by a fixed number $n \in \mathbb{N}$ of samples stored in a data table, $t_k \propto nt_s$, with $t_s = 1/30$ [s] being the sampling time of the UAV.

Algorithm 1 describes how to get the delayed data from the quadrotor. Note that given an n , which represents an index of the data history matrix, the quadrotor controller receives delayed information only when the elapsed time is greater than the delay. If no delay is set, then the robot receives the updated data. The Algorithm 1 initializes the variables of interest, a representation of the robot as an object, a reference scalar for the time delay n , a data matrix where relevant information such as UAV pose and velocities will be stored, an index k that will be incremented at each iteration for comparison in relation to n , and the current time of the control loop, which guarantees real-time operation. When initializing the mission, the code checks whether the current time is greater than the time delay. If so, the current position and velocity are considered to be delayed, if not, the robot is considered to receive and send current information. Computationally speaking, this avoids accessing non-existent slots in the data array. After this verification step, the data is sent to the control system that will calculate its action by sending control signals to the robot's dynamic model and observing its behavior. Performance indices are calculated for analysis after the end of the mission. All the data of interest is stored in the navigation history array (Hist). Finally, the control loop repeats until the maximum time stipulated for the task execution is reached.

B. Controller Tuning in Parameter Space

Control design from the parameter space is a widely used approach in robust control applications [15]. The technique

consists of designing a control system that fits some previously defined stability and/or performance specifications, carrying out a study of how the controlled plant behaves in the face of changes in the controller parameters [24]–[27]. The objective is to find a controller that behaves satisfactorily even in the presence of anomalous system variations, unmodeled

Algorithm 1: Acquisition of Time-Delayed Data [23]

```

Data:  $n \in \mathbb{N}$ ; // delayed info index
Hist; // data matrix
 $k$ ; // Initialize Counter
 $t_{ctrl}$ ; // Initialize control loop timer
Result: Robot behavior for a given time-delay ( $nt_s$ ).
while  $t < t_{max}$  do
  if  $t_{ctrl} > t_s$  then
     $t_{ctrl} \leftarrow 0$ ; // Reset control loop timer
    if  $k > n$  then
       $\mathbf{x} \leftarrow \text{Hist.Position}(k - n)$ ;
       $\dot{\mathbf{x}} \leftarrow \text{Hist.Velocity}(k - n)$ ;
    else
       $\mathbf{x} \leftarrow \text{Current Position}$ ;
       $\dot{\mathbf{x}} \leftarrow \text{Current Velocity}$ ;
    end
     $\tilde{\mathbf{x}} \leftarrow \mathbf{x}_d - \mathbf{x}$ ,  $\dot{\tilde{\mathbf{x}}} \leftarrow \dot{\mathbf{x}}_d - \dot{\mathbf{x}}$ ;
     $\mathbf{u}_d \leftarrow \tilde{\mathbf{x}}(t - t_k)$ ; // Delayed input to control
    signal as in Figure 3
    Numerical Integration to obtain the Reference State;
    UAV Dynamic Model;
    Calculation of the Performance Indices;
    Hist  $\cup$  Current UAV Data;
     $k \leftarrow k + 1$ ;
  end
end

```

parameters or plant uncertainties. Under the preset conditions, the stabilization at time 30 s, which corresponds to half-time of the mission, is considered satisfactory, with performance metrics less than $30 \times$ IAE and $50 \times$ ITAE. As well as limiting the modulus of the instantaneous error, which must be smaller than the initial error, prevents the robot from oscillating with increasing amplitudes around the target point, making the system unstable. After all, it rules out situations where the current position error becomes larger than the initial error of the task.

The purpose of this work differs slightly from the purposes of robust control design; however, a similar procedure is applied. The objective is to analyze the nonlinear control parameter space used for a set of predefined convergence and performance requirements. Hence, verify that the currently used control gains takes the control specifications.

To perform this analysis, a grid search is performed in a region that encompasses all the used gains. Multiple combinations of proportional and derivatives gains are tested to verify whether the resulting closed-loop system would meet the following requirements:

- The positioning error of less than 5 [m] (due to the position of the target point);
- IAE (Integral Absolute Error) and ITAE (Integral Time Absolute Error) performance indexes, respectively, lower than 30 and 50 times the no-delay case;
- The maximum overshoot smaller than the initial error.

Such requirements avoid selecting gains that generate initial

- $\mathbf{x}_d, \dot{\mathbf{x}}_d, \ddot{\mathbf{x}}_d \rightarrow$ target position, and desired velocities and accelerations
- $\mathbf{x}, \dot{\mathbf{x}}, \ddot{\mathbf{x}} \rightarrow$ current position, velocities and accelerations
- $\tilde{\mathbf{x}}, \dot{\tilde{\mathbf{x}}} \rightarrow$ current position and velocity errors
- $\mathbf{x}(t - t_k), \dot{\mathbf{x}}(t - t_k) \rightarrow$ delayed position and velocities
- $K_p, K_d \rightarrow$ proportional and derivative gains

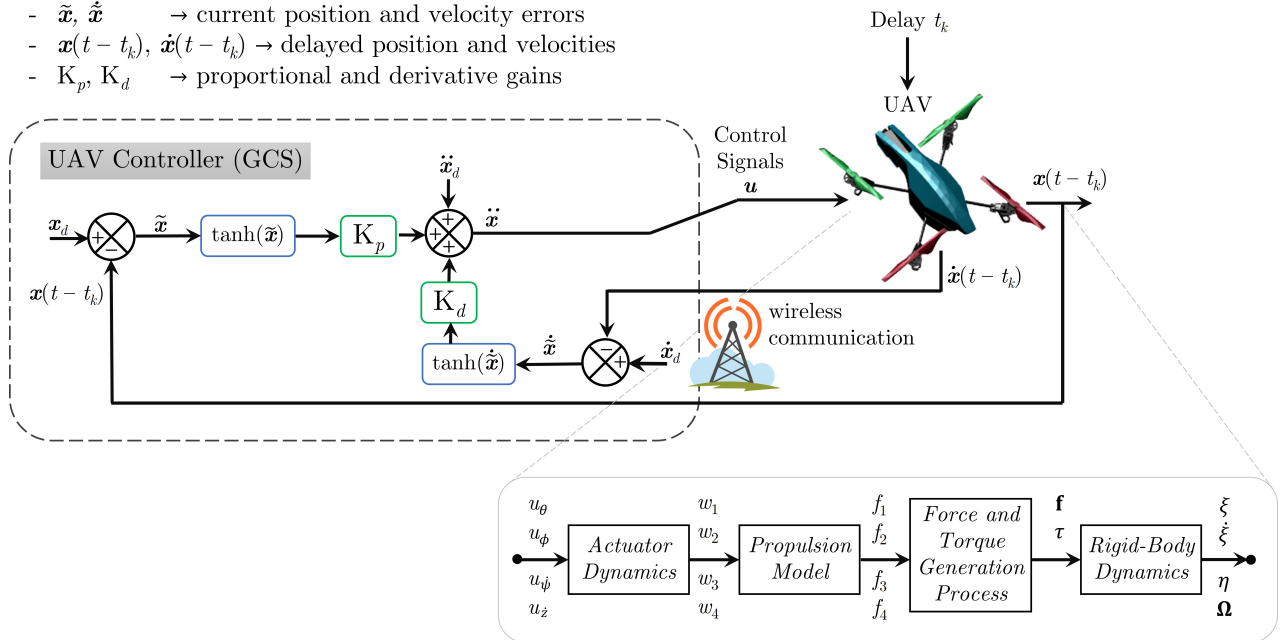


Fig. 3. Controller model sending/receiving data to/from the UAV after delay t_k . The robot communicates with the GCS via a wireless link, sending information regarding its current state, battery level data, camera images, etc.; and receives motion command signals. The transport delay is inserted due to the imperfection of the communication channel. Thus, the sending/receiving of information is compromised and may suffer packet loss and delay. The block diagram describing the dynamic model of the aerial robot is indicated in the lower right corner of the image (inside the gray square) as presented by Brandao *et al.* in Reference [17].

errors high enough to make the task infeasible. Also, they ignore cases where the robot does not reach the point, approaches very slow motion, reaches the desired point and then starts oscillating with growing amplitudes.

The range of the parameters are depicted in Table I. They enable a three-dimensional analysis, indicating under which conditions the system will remain stable and successfully accomplish the mission.

TABLE I
CONTROL PARAMETERS FOR THE NUMERICAL EXPERIMENTS.

Parameter	Range	Adopted Value
$\mathbf{K}_p [s^2]$	[0.05, 0.75]	0.50
$\mathbf{K}_d [s]$	[0.05, 1.00]	0.85
$t_k [s]$	[0.00, 1.25]	0.00

C. Performance, Convergence and Stability

The controller performance is analyzed in two ways: graphically, as a function of the parameters adopted, and mathematically, by the performance metrics in transient and permanent regimes during the execution of the mission. Such data also allow evaluating and estimating the energy consumption associated with the controller effort so that the asymptotic convergence is reached in the control objectives.

If the drone exhibits divergent oscillatory behavior, then the response is considered unstable. Otherwise, if responses have damped behavior, regardless of the time required for the drone to reach the steady-state, they are considered stable.

The IAE and ITAE performance indexes are used to evaluate the controller under each preset parametric condition. They are computed respectively by

$$IAE = \int_0^{t_f} \|\tilde{\mathbf{x}}\| dt \quad (1)$$

and

$$ITAE = \int_0^{t_f} t \|\tilde{\mathbf{x}}\| dt. \quad (2)$$

Both accumulate the position error over time. However, IAE provides information about how fast the robot reached the desired point, while ITAE evaluates the response in a permanent regime.

Another index adopted for comparing controllers is the integral of the absolute control signal (IACS), which allows us to evaluate the amplitude of signal sent by the controller over time, thus giving indications about the energy consumption associated with the task to be performed, for the analyzed controller. This index is given by

$$IACS = \int_0^{t_f} \|\mathbf{u}\| dt. \quad (3)$$

IV. SIMULATED RESULTS AND DISCUSSION

This section presents the results for positioning tasks subject to time delays. The temporal evolution of the UAV's posture is depicted during the delay in sending and receiving information. The performance indices help in conclusions about the

simulations performed according to the predefined parameters in view of the UAV response. Comparison of the results emphasizes the best responses and cases that reached the desired point in the specified time.

A. Simulation Setup

AuRoRA simulator is mobile robotics framework hosted on MATLAB[®] that runs the entire implementation. During the experiments, the adopted sampling time is $t_s = 1/30$ s, which the NavData package is shared with the AR.Drone Parrot 2.0, the experimental setup platform, whose parameters are shown in Table II (additional info can be found in [28]).

TABLE II
ARDRONE 2.0 MODEL PARAMETERS FOR THE NUMERICAL EXPERIMENTS.

High-level Model	Low-level Model
$m = 0.380$ [kg]	$\phi_{\max} = 25$ [°]
$k_1 = 0.178$ [m]	$\theta_{\max} = 25$ [°]
$k_2 = 0.029$ [Nms ²]	$\dot{\psi}_{\max} = 10$ [°/s]
$I_{xx} = 9.57 \times 10^{-3}$ [kgm ²]	$\dot{z}_{\max} = 0.6$ [m/s]
$I_{yy} = 18.57 \times 10^{-3}$ [kgm ²]	$k_{d\phi} = k_{d\theta} = 1$ [V/rad]
$I_{zz} = 25.55 \times 10^{-3}$ [kgm ²]	$k_{p\phi} = k_{p\theta} = 10$ [Vs/rad]
$I_{xy} = I_{yx} = 0$ [kgm ²]	$k_{d\psi} = 0.01$ [V/rad]
$I_{xz} = I_{zx} = 0$ [kgm ²]	$k_{p\psi} = 15$ [Vs/rad]
$I_{yz} = I_{zy} = 0$ [kgm ²]	$k_{dz} = 0.01$ [V/m]
	$k_{p\dot{z}} = 0.01$ [Vs/m]

To excite the dynamics of the UAV, a regulation task is required. For the step response here analyzed, initially, the drone starts at $\mathbf{d} = [0 \ 0 \ 0.75]^\top$ m, which is its resting position, and then it receives its target position at $\mathbf{d}_d = [-2 \ -1 \ 2]^\top$ m. It is expected that large position errors and control input peaks are observed at the beginning of the experiment, i.e., the transient response. In contrast, as the UAV approaches the target, the control signals decrease and ultimately tend to zero. Hence, such behavior highlights the asymptotic convergence in closed-loop of the implemented underactuated nonlinear controller.

Assuming that the closed-loop control system is stable, it is expected that after reaching the target, the aircraft remains hovering, performing an anchored flight, since the position errors are (close to) zero.

To have a baseline for comparison purposes, the positioning test is performed first without delays. Then, for each simulation, the navigation data is delayed by an additional sampling period ($t_s = 1/30$ s) until it reaches 1.2 s, which corresponds to 36 cycles/iterations of the control loop.

Figure 4(a) illustrates the no-delay critically damped response performed by a quadrotor, during the regulation maneuver. Notice in Figure 4(b) that there is no overshoot in the position variables. All of them converge and remain at the desired values, in about 15 s. For this scenario, the performance indices computed are $IAE_{wtd} = 11.41$ and $ITAE_{wtd} = 30.04$. The subscript *wtd* refers to the adopted values shown in Table I, whose mission execution occurs without time-delay.

B. Parameter Space Analysis

Figure 5 shows the results of the analysis in parameter space in such a case for a range of gains and time delay. It illustrates

the scattering of gain values combined with the time delay. In Figure 5(a), the circles of different sizes and colors refer to the predefined stability (and convergence) and performance specifications. These are: absolute error less than 5 m (in blue), IAE less than 30 times the base value (in green), ITAE less than 50 times the base value (in red), error norm less than the initial error (in orange).

Whenever a pair of gains meets the system specifications, a circle is drawn. For ease of visualization, Figure 5(b) indicates all the times that the above conditions are met. To give an overview of the tests performed, Figure 5(c) gives a smooth three-dimensional view over the range of values tested that meet all preset conditions.

Table III presents the minimum and maximum values of the performance indices, taking into account the predefined set of gains and time-delays. Notice that the minimum values occurs for a navigation without time-delay, as expected. Nevertheless, the maximum values do not occur for the largest acceptable time-delay, in turn they happen for low values of proportional gain. This is justified by the slow response of the system, which takes time to reduce the position error, and thus causes

TABLE III
PERFORMANCE INDICATORS OBTAINED IN THE POSITIONING TASK.

	IAE		ITAE	
	min	máx	min	máx
value	4.48	29.60	7.94	426.66
t_{delay} [ms]	0.0	180.0	0.0	360.0
\mathbf{K}_p	0.75	0.10	0.75	0.50
\mathbf{K}_d	0.65	0.60	0.55	0.70

the value of the performance indicators to increase. Finally, it is important to point out that for certain values of time-delay, there are no feasible gain combinations that can accomplish the task.

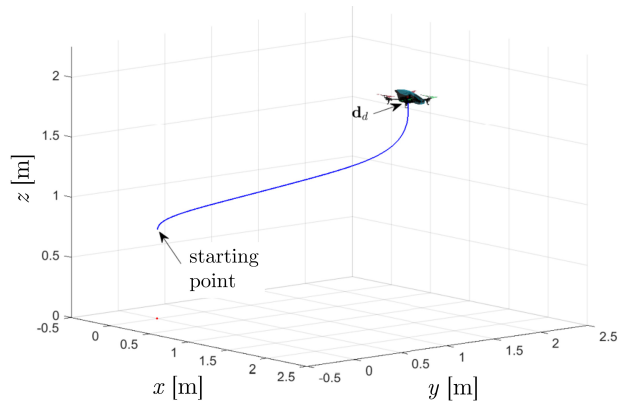
All the sets of gains and delays shown in Figure 5(c) keep the system stable, although some markings may be missing in the regions near the origin. For these cases, where the gains are small (range 0.05–0.20), the quadrotor receives relatively small control signals and consequently its response is slow. This makes the performance indices large at the end of the set simulation time. In other words, despite convergence in the permanent regime, the quadrotor takes a long time to mitigate the position error.

The gains used in the numerical simulations are $\mathbf{K}_p = 0.5$ and $\mathbf{K}_d = 0.85$. Note that they fall within the region formed by the specifications. By assuming the possibility of time delays, a simple and efficient way to overcome this is to look at the volume of Figure 5 and assign a new set of gains that meet this condition. It is worth noting that the gains can be updated before starting an experiment if there is an estimate available for maximum time-delay or through the continuous observation of the communication channel between the quadrotor and the GCS. In summary, if the parameters are in this volume, then the robot will accomplish the mission, respecting the preset conditions, in a smooth and stable manner.

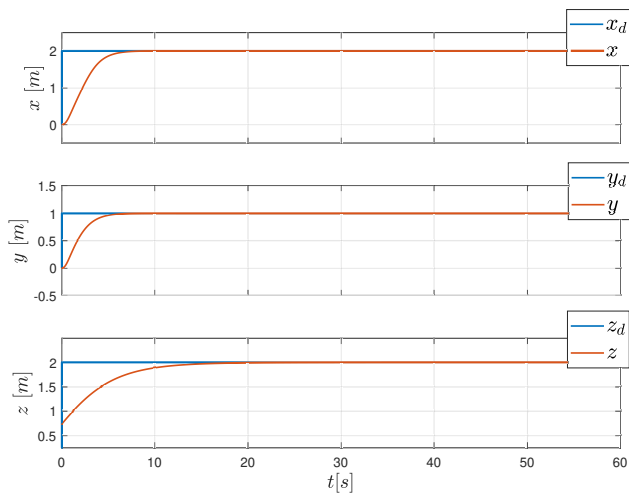
The analysis of the parameter space also points to an evaluation of which feature enhances or compromises navigation. In other words, the volume allows a discussion about the quadrotor's behavior as a function of increased or decreased gain and delay. It can be observed that the volume tends to assume a polyhedral profile, close to a triangular pyramid. This is because for high gains, despite the search for a fast and abrupt response, the consequence is saturation of the control signals. This justifies the concentration of valid gains in the vicinity of the origin. Under the presence of time delay, the quadrotor tends to present an unstable oscillatory response, the greater the delay. Hence, to ensure stability, the immediate solution is to reduce the gains.

C. Case Study and Summary of the Best Results

Given the quadrotor model used throughout this work, the next examples illustrate the behavior of the robot, when changing gains and time-delay, during mission execution. In the first scenario, the proportional and derivative gains respectively equal to $\mathbf{K}_p = 0.2$ and $\mathbf{K}_d = 0.5$ were adopted, while the communication delay initially starts at 60ms, increases to 300ms and ends at 800ms.



(a) 3-d view of the path traveled.



(b) Temporal evolution of the position.

Fig. 4. Quadrotor performing a positioning task without considering time-delay in the communication link.

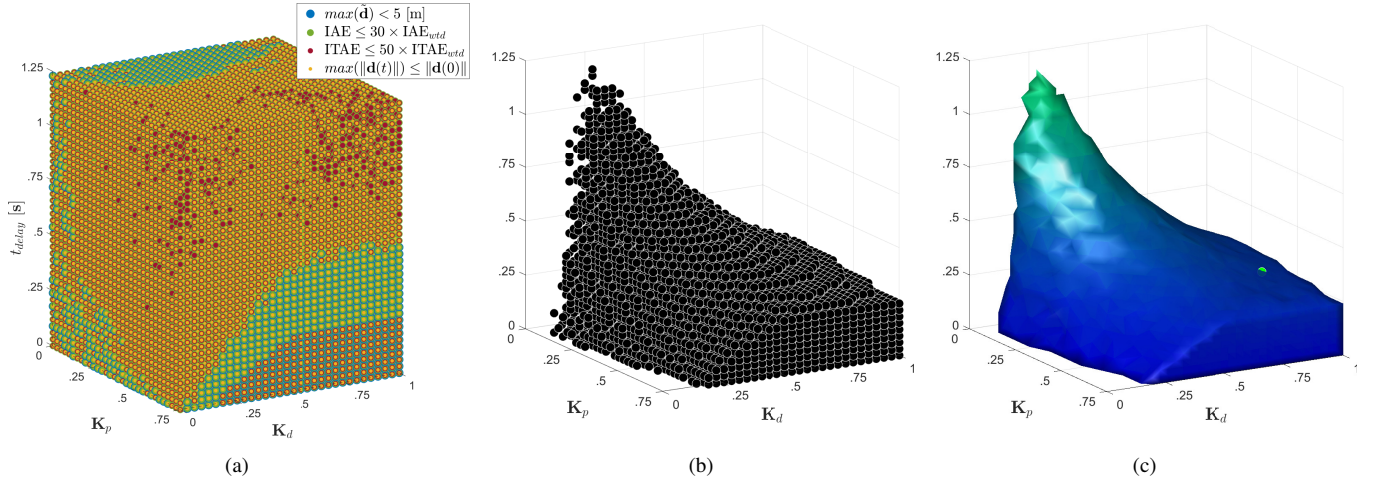


Fig. 5. Intersection of specifications in three-dimensional parameter space. (a) Representation of performance specifications. Each circle represents a set of gains and delays, and the colors in each circle represent a particular specification, as depicted in the legend. (b) Gains that satisfy all conditions for some delay. Each black sphere represents the intersection of all satisfied performance specifications. (c) Convex-hull volume of the satisfied performance specifications.

Figure 6 presents the temporal variations of the robot's position. Note that for the 60 and 300 ms delays, the quadrotor response does not change noticeably. In both cases, the drone reaches the permanent regime in about 20 seconds of simulation. In fact, these cases are predicted within the volume found in the analysis in parameter space, Figure 5(c). Thus, for these time delays, the selected gains satisfy the design specifications.

Analyzing the insertion of the delay of 800 ms, it is noticed that the pair of gains does not satisfy any of the restrictions. Consequently, as they are not part of the volume, the quadrotor exhibits undesired behavior. In fact, despite converging in the z direction, the quadrotor oscillates after 30 s of simulation, in the x and y directions. In this work, this fact is labeled as unstable and divergent.

Table IV gives a comparative description for the cases with the same gains and different time-delays. Note that for the

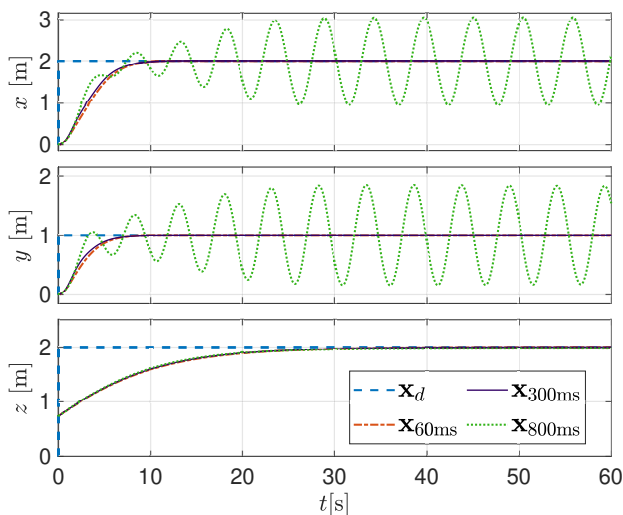


Fig. 6. Behavior of the quadrotor when performing the positioning task. Temporal variation of the position for $t_k = 60, 300$ and 800 [ms].

configuration outside the volume specified by Figure 5(c), the growth of the performance indices indicate the increase in the error variation, and especially, in the energy consumption required by the quadrotor, due to the permanent regime error. This last one computed by the integral of absolute value of the control signals.

Table V summarizes the best gains for the lowest IAE and ITAE. In other words, for the set of analyzed values, Table V shows the gain values for the simulations that obtained either the lowest value of IAE, or the lowest value of ITAE, having as reference the communication delay. Note, that the gains for the no-delay case are different when the IAE or ITAE index is prioritized. This analysis is relevant because they are directly related to the type of mission, i.e., if it is a positioning one, observe the IAE; if a tracking one, the ITAE. In fact, it is also possible to infer that as the time delay in sending and receiving information increases, the best results are obtained reducing the gain values. This is observed since small gains (K_p, K_d) provide control signals with increasingly smaller amplitudes, causing the robot response to be slower, and compensate for some of the information delay. Thus, despite taking longer to execute its mission, the robot executes it in a stable manner, preventing oscillations.

Finally, in a general view, as the delay increases, to keep performance rates low, and consequently maintaining the system stable, gains need to be reduced, as can be seen in Table V. However, with this, the robot needs a longer

TABLE IV
SUMMARY OF PERFORMANCE INDICES FOR THE POSITIONING TASK.

Time-delay (ms)	IAE	ITAE	IASC	Delayed Samples
0	19.6017	100.3511	1.5899	0
60	19.5840	101.7891	1.5939	2
300	19.7473	101.3777	1.6771	10
800	71.0960	1960.8015	28.3404	27

time to perform the task and the performance indices grow faster, since the error will take longer to converge to zero. Consequently, the robot moves more slowly and manages to fulfill the mission within the specifications. Such information can also be concluded from the volume obtained in Figure 5(c), in which it can be seen that increasing the time delay only makes it possible to meet the proposed requirements if the gains decrease, thus causing an increasingly slower movement.

V. CONCLUDING REMARKS

This work aims to estimate the acceptable limit of feedback delay for a quadrotor, from the analysis of the effects of inserting the delay at the communication link between the UAV with the GSC, as a function of the variation of two control gains. The stable convergence of the robot states during the execution of a positioning mission was analyzed, in a three-dimensional search space.

The best gain configuration, in the no-delay flight condition, was used as the baseline for comparison purposes. Thereafter, for delays up to 1.2 seconds, corresponding to 40 sampling periods of the UAV, pairs of gains were sought, within a preset range of values, and determined as a function of the

IAE or ITAE performance indices. Finally, a mapping of the gains that ensure convergence in executing the task in a timely manner was performed, and the acceptable delay interval can be selected and the behavior of the robot can be analyzed in the parameter space for automatic controller calibration.

Although it is possible to verify the stability of the system when subjected to parametric uncertainties or amplitude-limited perturbations, a robustness and phase/margin gain analysis of the second-order closed-loop system is beyond the scope of this paper, and remains a suggestion for future work.

ACKNOWLEDGMENTS

The authors thank to CNPq - Conselho Nacional de Desenvolvimento Científico e Tecnológico, to FAPES - Fundação de Amparo à Pesquisa e Inovação do Espírito Santo, to CAPES - Coordenação de Aperfeiçoamento de Pessoal de Nível Superior, and to FAPEMIG - Fundação de Amparo à Pesquisa do Estado de Minas Gerais, for the support given to this research.

REFERENCES

- [1] S. Al Issa and I. Kar, "Design and implementation of event-triggered adaptive controller for commercial mobile robots subject to input delays and limited communications," *Control Engineering Practice*, vol. 114, p. 104865, 2021.
- [2] Z. Qiao, J. Zhang, X. Qu, and J. Xiong, "Dynamic self-organizing leader-follower control in a swarm mobile robots system under limited communication," *IEEE Access*, vol. 8, pp. 53 850–53 856, 2020.
- [3] Z. Wang, H.-K. Lam, B. Xiao, Z. Chen, B. Liang, and T. Zhang, "Event-triggered prescribed-time fuzzy control for space teleoperation systems subject to multiple constraints and uncertainties," *IEEE Transactions on Fuzzy Systems*, 2020.
- [4] Y. Ji and Y. Gong, "Adaptive control for dual-master/single-slave nonlinear teleoperation systems with time-varying communication delays," *IEEE Transactions on Instrumentation and Measurement*, 2021.
- [5] T. Muskardin, A. Coelho, E. R. Della Noce, A. Ollero, and K. Konrad, "Energy-based cooperative control for landing fixed-wing uavs on mobile platforms under communication delays," *IEEE Robotics and Automation Letters*, vol. 5, no. 4, pp. 5081–5088, 2020.
- [6] H. Singh, M. Panzirsch, A. Coelho, and C. Ott, "Proxy-based approach for position synchronization of delayed robot coupling without sacrificing performance," *IEEE Robotics and Automation Letters*, vol. 5, no. 4, pp. 6599–6606, 2020.
- [7] S. Roy, I. N. Kar, and J. Lee, "Toward position-only time-delayed control for uncertain euler-lagrange systems: Experiments on wheeled mobile robots," *IEEE Robotics and Automation Letters*, vol. 2, no. 4, pp. 1925–1932, 2017.
- [8] Y. Xu, D. Li, D. Luo, and Y. You, "Affine formation maneuver tracking control of multiple second-order agents with time-varying delays," *Science China Technological Sciences*, vol. 62, no. 4, pp. 665–676, 2019.
- [9] A. Zhang, D. Zhou, M. Yang, and P. Yang, "Finite-time formation control for unmanned aerial vehicle swarm system with time-delay and input saturation," *IEEE Access*, vol. 7, pp. 5853–5864, 2018.
- [10] Y. Kali, J. Rodas, R. Gregor, M. Saad, and K. Benjelloun, "Attitude tracking of a tri-rotor uav based on robust sliding mode with time delay estimation," in *2018 International Conference on Unmanned Aircraft Systems (ICUAS)*. IEEE, 2018, pp. 346–351.
- [11] Y. Kartal, K. Subbarao, N. R. Gans, A. Dogan, and F. Lewis, "Distributed backstepping based control of multiple uav formation flight subject to time delays," *IET Control Theory & Applications*, vol. 14, no. 12, pp. 1628–1638, 2020.
- [12] J. Zhang, X. Zhu, and Z. Zhou, "Design of time delayed control systems in uav using model based predictive algorithm," in *2010 2nd International Asia Conference on Informatics in Control, Automation and Robotics (CAR 2010)*, vol. 1. IEEE, 2010, pp. 269–272.
- [13] J. M. Hansen, T. I. Fossen, and T. A. Johansen, "Nonlinear observer for ins aided by time-delayed gnss measurements: Implementation and uav experiments," in *2015 International Conference on Unmanned Aircraft Systems (ICUAS)*. IEEE, 2015, pp. 157–166.

TABLE V

MISSION ANALYSIS BASED ON THE PERFORMANCE INDICES. THE TABLE SHOWS THE BEST GAINS ACHIEVED FOR A GIVEN TIME DELAY, TAKING INTO ACCOUNT THE LOWEST IAE OR THE LOWEST ITAE.

t_k [s]	Observing the lowest IAE				Observing the lowest ITAE			
	K_p	K_d	IAE	ITAE	K_p	K_d	IAE	ITAE
0.00	0.75	0.60	4.453	7.985	0.75	0.55	4.488	7.896
0.03	0.75	0.70	4.535	8.355	0.75	0.70	4.535	8.355
0.06	0.75	0.70	4.625	8.474	0.75	0.60	4.629	8.241
0.09	0.75	0.70	4.671	8.504	0.75	0.70	4.671	8.504
0.12	0.75	0.70	4.761	8.729	0.75	0.70	4.761	8.761
0.15	0.75	0.85	4.969	10.198	0.75	0.75	4.979	9.599
0.18	0.75	0.85	5.087	10.621	0.75	0.70	5.201	10.036
0.21	0.65	0.70	5.521	12.221	0.70	0.80	5.606	12.121
0.24	0.60	0.70	5.914	14.813	0.55	0.60	6.078	14.783
0.27	0.55	0.70	6.404	18.936	0.50	0.55	6.549	17.336
0.30	0.50	0.60	6.857	21.387	0.45	0.55	6.953	19.792
0.33	0.45	0.60	7.311	24.729	0.40	0.45	7.683	23.380
0.36	0.40	0.60	7.896	28.501	0.35	0.50	8.199	28.222
0.39	0.35	0.45	8.403	29.557	0.35	0.45	8.403	29.557
0.42	0.35	0.50	8.762	36.281	0.30	0.45	9.174	35.694
0.45	0.30	0.40	9.476	38.167	0.30	0.40	9.476	38.167
0.48	0.30	0.50	9.915	49.354	0.25	0.35	10.459	46.099
0.51	0.25	0.35	10.728	48.875	0.25	0.35	10.728	48.875
0.54	0.25	0.45	10.969	54.639	0.25	0.45	10.969	54.639
0.57	0.40	0.25	11.509	67.037	0.25	0.40	11.509	67.037
0.60	0.20	0.35	12.453	68.244	0.20	0.35	12.453	68.244
0.63	0.20	0.30	13.195	78.087	0.20	0.30	13.195	78.087
0.66	0.20	0.45	14.105	108.045	0.10	0.40	17.061	31.202
0.69	0.20	0.40	14.277	119.549	0.20	0.35	16.329	107.581
0.72	0.15	0.40	16.619	127.101	0.15	0.35	18.120	125.228
0.75	0.15	0.30	16.726	114.459	0.15	0.30	16.726	114.459
0.78	0.15	0.30	15.792	113.239	0.15	0.30	15.792	113.239
0.81	0.15	0.25	19.892	193.208	0.15	0.30	20.937	153.430
0.84	0.15	0.40	20.409	280.301	0.10	0.20	21.429	207.520
0.87	0.15	0.30	20.883	261.572	0.10	0.30	21.108	230.146
0.90	0.10	0.25	21.249	214.854	0.10	0.25	21.249	214.854
0.93	0.10	0.20	21.472	211.923	0.10	0.20	21.472	211.923
0.96	0.10	0.25	21.401	215.834	0.10	0.25	21.401	215.834
0.99	0.10	0.30	24.583	242.933	0.10	0.30	24.583	242.933
1.02	0.10	0.30	22.339	233.851	0.10	0.30	23.859	218.868
1.05	0.10	0.25	21.912	224.999	0.10	0.30	22.339	233.851
1.08	0.10	0.25	24.638	292.662	0.10	0.25	21.912	224.999
1.11	0.10	0.25	23.207	274.077	0.10	0.25	24.638	292.662
1.14	0.10	0.25	24.550	299.089	0.10	0.25	23.207	274.077
1.17	0.10	0.25	29.498	394.128	0.10	0.25	29.498	394.128
1.20	0.10	0.25	27.313	424.444	0.10	0.25	27.316	424.444

- [14] L. Han, X. Dong, Q. Li, and Z. Ren, "Formation tracking control for time-delayed multi-agent systems with second-order dynamics," *Chinese journal of aeronautics*, vol. 30, no. 1, pp. 348–357, 2017.
- [15] Fialho Coelho, Andre, "System Identification and Parameter Space Control Design for a Small Unmanned Aircraft," <https://elib.dlr.de/114216/>, 2017, online; accessed 10 January 2022.
- [16] L. V. Santana, A. S. Brandão, and M. Sarcinelli-Filho, "Outdoor way-point navigation with the ar. drone quadrotor," in *2015 International Conference on Unmanned Aircraft Systems (ICUAS)*. IEEE, 2015, pp. 303–311.
- [17] A. S. Brandão, M. Sarcinelli-Filho, and R. Carelli, "High-level underactuated nonlinear control for rotorcraft machines," in *2013 IEEE International Conference on Mechatronics (ICM)*. IEEE, 2013, pp. 279–285.
- [18] A. Hernandez, H. Murcia, C. Copot, and R. De Keyser, "Model predictive path-following control of an ar. drone quadrotor," in *Memorias del XVI Congreso Latinoamericano de Control Automatico, Proceedings*, 2014, pp. 618–23.
- [19] A.-R. Merheb, H. Noura, and F. Bateman, "Emergency control of ar drone quadrotor uav suffering a total loss of one rotor," *IEEE/ASME Transactions on Mechatronics*, vol. 22, no. 2, pp. 961–971, 2017.
- [20] S. Piskorski and N. Brulez, "Ar. drone developer guide parrot. sdk version 2.0," *tech. rep.*, 2012.
- [21] L. V. Santana, A. S. Brandão, and M. Sarcinelli-Filho, "Navigation and cooperative control using the ar. drone quadrotor," *Journal of Intelligent & Robotic Systems*, vol. 84, no. 1, pp. 327–350, 2016.
- [22] M. F. S. Rabelo, A. S. Brandão, and M. Sarcinelli-Filho, "Centralized control for an heterogeneous line formation using virtual structure approach," in *2018 Latin American Robotic Symposium, 2018 Brazilian Symposium on Robotics (SBR) and 2018 Workshop on Robotics in Education (WRE)*. IEEE, 2018, pp. 135–140.
- [23] L. Fagundes-Junior, M. Canesche, R. Ferreira, and A. Brandão, "A nonlinear uav control tuning under communication delay using hpc strategies in parameters space," in *Anais do XXII Simpósio em Sistemas Computacionais de Alto Desempenho*. SBC, 2021, pp. 228–239.
- [24] D. D. Siljak, "Parameter space methods for robust control design: a guided tour," in *1988 American Control Conference*. IEEE, 1988, pp. 783–783.
- [25] J. Geromel, P. D. Peres, and J. Bernussou, "On a convex parameter space method for linear control design of uncertain systems," *SIAM Journal on Control and Optimization*, vol. 29, no. 2, pp. 381–402, 1991.
- [26] S. Zhu, S. Y. Gelbal, X. Li, M. R. Cantas, B. Aksun-Guvenc, and L. Guvenc, "Parameter space and model regulation based robust, scalable and replicable lateral control design for autonomous vehicles," in *2018 IEEE conference on decision and control (CDC)*. IEEE, 2018, pp. 6963–6969.
- [27] F. Ma, J. Wang, Y. Yu, L. Wu, Z. Liu, B. Aksun-Guvenc, and L. Guvenc, "Parameter-space-based robust control of event-triggered heterogeneous platoon," *IET Intelligent Transport Systems*, 2021.
- [28] T. Krajník, V. Vonásek, D. Fišer, and J. Faigl, "Ar-drone as a platform for robotic research and education," in *International conference on research and education in robotics*. Springer, 2011, pp. 172–186.



Leonardo A. Fagundes, Jr., received the B.S. degree in electrical engineering from the Federal University of Viçosa, Brazil, in 2020. He is currently pursuing the M.Sc. degree in computer science with the Federal University of Viçosa. His research interest includes control of multi-robot systems applied to aerial robots navigation and communication systems.



André F. Coelho received the B.E. degree in Control and Automation Engineering from the Federal Fluminense Institute (IFF), Brazil and the M.Sc. degree in Electrical Engineering from the Federal University of Rio de Janeiro (UFRJ), Brazil, in 2018 and 2019, respectively. In 2014 and 2015 he was a visiting student at the University of Colorado Boulder, USA. In 2019 he joined the the Institute of Robotics and Mechatronics at the German Aerospace Center (DLR) as a research scientist. Since 2021 he has been enrolled as a PhD candidate at the Faculty of Electrical Engineering, Mathematics and Computer Science (EEMCS) at the University of Twente, The Netherlands. His current research interests include teleoperation and whole-body control of aerial manipulators. He recently participated in the AEROARMS H2020 project and other research activities with the Flying robots and the Teleoperation Control groups. His current research interests include teleoperation and whole-body control of aerial manipulators.



Daniel K. D. Villa graduated in Electrical Engineering from the Federal University of Viçosa (2014). He carried out his final project in the area of Control and Automation. He received his Master degree in Agricultural Engineering, also from the Federal University of Viçosa, working in the area of Drying of Agricultural Products with the development of an air conditioning system applied to the drying and storage of agricultural products. He is currently a lecturer of the lato sensu postgraduate course, distance modality, in Automation and Control of

Agricultural and Industrial Processes offered by the Department of Electrical Engineering (UFV) in partnership with CEAD (UFV). He is currently a Ph.D. student at Federal University of Espírito Santo (UFES).



Mário Sarcinelli-Filho received the B.S. degree in electrical engineering from the Federal University of Espírito Santo, Brazil, in 1979, and the M.Sc. and Ph.D. degrees in electrical engineering from the Federal University of Rio de Janeiro, Brazil, in 1983 and 1990, respectively. He is currently a Professor with the Department of Electrical Engineering, Federal University of Espírito Santo and a Researcher with the Brazilian National Council for Scientific and Technological Development (CNPq). He has also advised 20 Ph.D. students and 26 M.Sc. students.

He has coauthored more than 65 journal articles, 350 conference papers, and 17 book chapters. His research interests include non-linear control, mobile robot navigation, and coordinated control of ground and aerial robots. He is also a member of the Brazilian Society of Automatics and of the Editorial Board of the *Journal of Intelligent & Robotic Systems*, published by Springer.



Alexandre S. Brandão holds a degree in Electrical Engineering from the Federal University of Viçosa (UFV, 2006), a Master's and Ph.D. in Electrical Engineering from the Federal University of Espírito Santo (UFES, 2008 and 2013), with emphasis on Automation. In 2014, he received from the Instituto de Automática (INAUT) of the National University of San Juan, Argentina, his Ph.D. in Control Systems Engineering. Since 2010, he is with the Department of Electrical Engineering, Federal University of Viçosa, Brazil, and head of the Núcleo de Especialização em Robótica (NERo). Since 2016, he is with the Post-graduate program in Electrical Engineering at UFES, and in Computer Science at UFV. His research interest is linear and nonlinear control, human-machine interaction, navigation and formation control of unmanned aerial and terrestrial vehicles.